Planar Lipid Bilayers (BLMs) and their Applications
H.T. Tien and A. Ottova-Leitmannova (Editors)

Chapter 10

Membrane-Macromolecule Interactions and their Structural Consequences

S. May[a] **and A. Ben-Shaul**[b]

[a]Institut für Molekularbiologie, Friedrich-Schiller-Universität Jena,
Winzerlaer Str. 10, Jena 07745, Germany

[b]Department of Physical Chemistry and the Fritz Haber Research Center,
The Hebrew University, Jerusalem 91904, Israel

1. INTRODUCTION

The lipid bilayer, constituting the central structural component of biological membranes, is a *flexible, self-assembled, two-dimensional fluid mixture*. Each of these bilayer characteristics, separately and more often jointly with others, plays a crucial role in the interaction between biomembranes and biological macromolecules, such as integral or peripheral proteins and DNA. Being *flexible* (or "elastic") with respect to bending deformations, the bilayer can respond to interactions with both peripheral and intrinsic macromolecules through local or even global variation of its curvature. Changes in membrane area (and hence thickness) are also possible, but usually involve a higher energetic cost. A local change in membrane structure occurs, for example, when a hydrophobic α-helical peptide is inserted into a lipid bilayer whose thickness does not match its length. By locally changing its curvature (and thickness) around the incorporated peptide the lipid bilayer minimizes the exposure of hydrophobic (protein or lipid) moieties to water [1].

A more drastic, global, change in membrane curvature may occur, for instance, when a double stranded DNA molecule adsorbs onto a lipid bilayer composed of cationic and neutral lipids [2]. Driven by the electrostatic attraction between the negatively charged DNA and the positively charged lipids, the bilayer tends to wrap around the DNA, paying the energetic toll of membrane bending deformation. This bilayer-coated DNA complex (later referred to as the "spaghetti"-like complex [3]) is usually metastable with respect to other

DNA-lipid complexes. In general, mixing DNA and cationic (liposomal) bilayers results in the spontaneous formation of periodic composite phases of lipid and DNA, characterized by either lamellar or hexagonal symmetry [4,5]; (see Fig. 2 in Sec. 3). As in the ordinary lamellar lipid phase (L_α), the lamellar complex phase (L_α^c) consists of a stack of bilayers, but with monolayers of parallel DNA strands sandwiched between them. Other lipid mixtures end up forming hexagonal complexes (H_{II}^c), consisting of double stranded DNA's intercalated within the aqueous tubes of the inverse hexagonal lipid phase (H_{II}). The formation of such lipid-DNA complexes exhibits both the *fluidity* and *self-assembly* properties of lipid mixtures.

The cationic lipids in the L_α^c complex tend to concentrate in the vicinity of the DNA. Similar phenomena occur when, say, basic proteins adsorb onto lipid membranes containing a small fraction of acidic lipids. Driven by electrostatic attraction to the macromolecule, the charged lipids diffuse into the interaction zone, now paying the (tolerable) toll of lateral *demixing* entropy. Clearly, this ability of the membrane to "optimize" its interaction with a neighboring macromolecule, is possible because the bilayer is a two-dimensional *fluid mixture*.

In forming the H_{II}^c complex with DNA, the lipid bilayer undergoes a much more dramatic change than a "simple" bending or stretching deformation. This process is a real, first order, thermodynamic phase transition. An analogous, lamellar-to-inverse hexagonal, lipid phase transition can be induced by the incorporation of short hydrophobic peptides into lipid bilayers [6] (see below). Again, the occurrence of these, and various other morphological transformations and phase transitions in lipid systems, are direct consequences of the fact that lipid molecules in water spontaneously organize in *self-assembling* aggregates.

Belonging to the wider class of amphiphilic molecules, lipids in aqueous solution exhibit a rich variety of self-assembled aggregates and ordered phases [7]. The aggregation geometry of ultimate biological importance is, of course, the planar bilayer. Other familiar lipid assemblies include the inverse-hexagonal (H_{II}) phase mentioned above, as well as a multitude of cubic and micellar phases. The spontaneous formation of H_{II}^c complexes by adding DNA into a solution of vesicles, i.e., *planar lipid bilayers*, demonstrates how interacting macromolecules can modify the self-assembly characteristics of the lipid species. Still, since only certain mixed lipid bilayers end up forming hexagonal complexes while others remain lamellar, there must be some intrinsic preference of the lipid constituents for one packing geometry over the other. Indeed, the propensity of lipids and other amphiphiles to self-assemble into one of many possible packing geometries, may be understood, at least qualitatively, by considering their "molecular shape" [8,9]. Most ionic surfactants, as well as certain lipids, like the single-tailed lyso-PC (phosphatidylcholine), comprise

a single hydrophobic tail and a relatively large polar head group. (The head group "size" is dictated by the range of the repulsive interaction with neighboring molecules. The interaction may be steric, electrostatic, etc.) The overall shape of such molecules may be depicted as a cone, suggesting that their optimal packing geometry is that of a highly curved aggregate, e.g., a spherical or cylindrical micelle, a notion corroborated by many experiments. Other lipids may be depicted as "inverted cones", with their head group positioned at the cone vertex. DOPE (dioleoylphosphatidylethanolamine) for instance. involves a relatively small head group and, like most phospholipids, a bulky double-chain tail. As expected, the preferred aggregation geometry of such molecules is the inverse hexagonal, H_{II}, or some other inverted (that is, "hydrocarbon-continuous" rather than "water-continuous") phase.

The molecular packing characteristics of most lipid species, DOPC (dioleoylphosphatidylcholine) to mention one example, are intermediate between the above two extremes. Namely, their head groups and tails are of comparable size. These molecules spontaneously assemble into planar bilayers. Recall, however, that two monolayers combine to form a bilayer only because a single monolayer in solution is unstable, owing to the high interfacial energy associated with exposing its hydrophobic surface to water. Yet, based only on molecular packing considerations we expect that most monolayers should possess a nonzero *spontaneous curvature* [10]. For instance, if inter-head group repulsion is stronger than tail-tail repulsion (imagine a "truncated cone" with the head group at its wider base) the monolayer will tend to curve "positively", i.e., with the head groups on the concave side. In forming a *planar* bilayer the two monolayers rid off the highly unfavorable hydrocarbon-water interfacial energy, paying a smaller yet nonzero curvature elastic energy associated with flattening the (spontaneously curved) monolayers. As we shall see below, this *elastic frustration* energy, plays a subtle yet crucial role in the phase behavior of membrane-macromolecule assemblies.

In our discussion so far we have emphasized the various modes in which a lipid bilayer can respond to interactions with biopolymers, implicitly assuming that the latter are rigid macromolecules. While not invariably so, in most interacting lipid-macromolecule systems the soft-mixed-fluid membrane is, indeed, considerably more amenable to structural modifications as compared to most proteins and certainly in comparison to DNA. Consistent with this notion we shall treat the interacting biopolymer as a rigid macromolecule of a given size and shape, as well as of given charge distribution in the case of DNA and charged proteins. Our goal is to present a simple, yet powerful, theoretical framework for treating the roles of membrane elasticity, its two-dimensional fluidity, and its ability to re-assemble in lipid-macromolecule interactions. As specific examples we shall consider lipid-DNA complexes and two types of

lipid-protein systems, exhibiting both local and global structural re-organization of the lipid matrix.

The theoretical description of membrane-macromolecule interaction involves two complementary aspects. First, on a 'molecular' (or 'local') level one has to calculate the interaction free energy between the macromolecule, e.g., an adsorbed or trans-membrane protein, and the lipid bilayer. This calculation should yield the interaction free energy as a function of the molecular and thermodynamic characteristics of the system such as membrane composition, protein size and charge and the ionic strength of the solution. Within this molecular-level theory, and using appropriate (typically mean-field like) approximations one may also account for macromolecule concentration effects, e.g., the variation of protein adsorption energy on the density of already adsorbed proteins. The second stage of the theoretical treatment involves the inclusion of the calculated interaction potential in a statistical-thermodynamic treatment of the membrane-macromolecule system. The phase behavior of this multi-component system is then derived by analyzing its (usually rather complicated) thermodynamic free energy.

The thickness of lipid bilayers, as well as typical diameters of proteins and DNA are all in the nanometer-range. This range defines the relevant length scale for lipid-macromolecule interactions, e.g., the range of elastic perturbations of lipid hydrocarbon chains by a trans-membrane protein, or the range of modulations in lipid composition induced by protein adsorption. Atomistic-level theories or computer simulations have proved useful in studying specific (e.g., protein-lipid) systems over a limited range of time and length scales [11]. At present they do not yet provide an efficient means for analyzing global, nanometer-range phenomena such as membrane curvature modulations or phase transitions following protein adsorption or insertion. Many interesting general questions can be answered using "mesoscopic-level" theories; e.g., how does the adsorption isotherm of basic proteins on acidic membrane vary with protein charge and size and the mole fraction of acidic membrane lipids, or, what is required from a lipid mixture in order to form hexagonal rather than lamellar DNA-lipid complexes. By mesoscopic-level theories we refer here to continuum models, based on expressing the free energy of the interacting system as an integral over locally varying contributions. In the present context we mainly refer to two rather simple and most useful theoretical tools. The phenomenological, Helfrich's, formalism of membrane elasticity, and the Poisson-Boltzmann (PB) theory for the electrostatic interaction between charged surfaces in ionic solutions. We find it appropriate to briefly recapitulate – in Sec. 2 – these tools before proceeding to discuss lipid-macromolecule interactions. Then, in Sec. 3 we shall discuss the major structural and thermodynamic characteristics of cationic lipid-DNA complexes, focusing on the coupling between electro-

static, elastic and compositional degrees of freedom of the lipid mixture. In Sec. 4 we shall discuss the electrostatic adsorption of charged proteins on oppositely charged membranes, emphasizing the role of lipid mobility and lateral adsorbate interactions. Sec. 5 is devoted to the interaction of membranes with integral, hydrophobic, proteins. Our goal here is to demonstrate how, on one hand, membrane lipids can mediate the interaction between embedded proteins, possibly leading to two-dimensional phase transitions and, on the other hand, how proteins can drive morphological phase transitions of lipid bilayers. A few comments pertaining to partially membrane-penetrating biopolymers are given in the final section.

2. ELASTIC AND ELECTROSTATIC FREE ENERGIES

2.1. Curvature elasticity

Lipid membranes are quite "soft" with respect to bending deformations. In contrast to that, changes in membrane thickness generally involve large deformation energies. Frequently, membrane deformations cannot be simply classified as pure bending or stretching deformations. This is the case, for instance, when a lipid bilayer is perturbed by the incorporation of either short or long trans-membrane proteins, as will be discussed in Sec. 5. Nevertheless, the principles of membrane curvature elasticity are essential for understanding membrane-macromolecule interaction phenomena. To this end let us consider a lipid bilayer of total, equilibrium, area A; ignoring area deformations we treat A as a constant. The equilibrium curvature of the symmetric bilayer, i.e., a bilayer composed of two identical monolayers is, of course, zero. However, as mentioned in the previous section, depending on the relative magnitude of lipid head group and tail interactions, the monolayers tend to adopt some nonzero equilibrium curvature, c_{eq}. Similarly a non-symmetric bilayer will also possess a nonzero equilibrium curvature.

A most useful expression for the elastic energy of lipid films (i.e., monolayers, bilayers or, in fact, any thin membrane) has been proposed by Helfrich [10]. Let R_1 and R_2 denote the local principal radii of curvature at some given point of the membrane, (hence $c_1 = 1/R_1, c_2 = 1/R_2$ are the corresponding principal curvatures), and da a small area element around this point. The curvature elastic free energy of the film can now be expressed in the form

$$F = \int_A da \left[\frac{k}{2}(c_1 + c_2 - c_0)^2 + \bar{k}c_1c_2\right] \tag{1}$$

where $k, \bar{k}$ and c_0 are material constants depending on the lipid composition of the film; k and $\bar{k}$ are elastic moduli known as splay modulus (or bending rigidity), and saddle-splay modulus, respectively. The bending rigidity of common

lipid layers is typically of order $k = 10\ k_BT$; with k_B denoting Boltzmann's constant, and T is the absolute temperature. It is much harder to measure or calculate the saddle-splay modulus $\bar{k}$. However, the Gauss-Bonnet theorem states that the second term in Eq. (1) represents a topological invariant, and is thus irrelevant whenever the topology is the lipid aggregate remains unaffected.

The constant c_0 in Eq. (1) is known as the *spontaneous curvature* and is closely related to the equilibrium curvature of the film, i.e., to the optimal packing curvature of the constituent lipids. More specifically, minimizing F with respect to c_1 and c_2 it is easy to show that at the equilibrium configuration of the membrane $c_1 = c_2 \equiv c_{eq} = kc_0/(2k + \bar{k})$. Another result which follows directly from Eq. (1) involves the curvature frustration energy associated with joining two monolayers to form a planar bilayer. This energy is always positive and given by $\Delta F_{frus} = 2kc_0c_{eq}A$. It may be compared with the surface energy associated with exposing the two hydrophobic surfaces of the separated monolayers to water; $\Delta F_{surface} = 2\gamma A$, with $\gamma \approx 10k_BT/\mathrm{nm}^2$ denoting the hydrocarbon-water surface energy. For typical monolayer parameters, $k \approx 10k_BT$ and $c_0 \approx c_{eq} \leq 1/(10\ \mathrm{nm})$ we find that $\Delta F_{surface}$ is at least two orders of magnitude larger than ΔF_{frus}, explaining why the bending frustration energy is a small penalty compared to the large energetic gain resulting from the association of two monolayers into a bilayer. Yet, the transition from the bilayer to the inverse hexagonal lipid geometry does not involve exposure of hydrocarbon tails to water, and the curvature frustration energy, though nominally small, becomes a crucial factor. This and other issues pertaining to membrane elasticity are further discussed in the following sections.

2.2. Electrostatic free energy

Given the electrostatic potential in a system containing macroions (e.g., charged membranes, proteins or DNA) in solution, one can calculate the electrostatic ("charging") energy for arbitrary macroion configurations. Interaction potentials between macroions, e.g., those depicted in Fig. 1, can then be derived by comparing the energies (actually free energies, see below) corresponding to different distances. In principle, from classical electrostatics we know that for any given distribution of charges, the electrostatic potential, $\Phi = \Phi(\mathbf{r})$, is determined by the solution of Poisson's equation. An exact treatment of a system such as in Fig. 1, assuming the macroions to be fixed in space, requires solving Poisson's equation for all possible distributions of the mobile ions. Then, after assigning each distribution its proper statistical weight one could derive the interaction free energy of this system. This can only be achieved through computer simulations. However, because of the long range nature of the Coulomb potential, and the high complexity of most systems of biological relevance, computer simulations are so far available only for a small number of model systems. A most useful alternative for studying electrostatically in-

teracting macroions in solution is provided by an approximate, "mean-field" approach, known as Poisson-Boltzmann (PB) theory [12]. All the electrostatic treatments in the following sections are in the spirit of PB theory.

Driven by Coulomb attractions, the mobile ions in solution tend to concentrate near oppositely charged (macroion) surfaces, thus lowering the electrostatic *energy* of the system. This tendency is opposed by the *entropic* penalty associated with any deviation of the local ion densities, $n_i(\mathbf{r})$, from their bulk (i.e., far from any charge surface) values, n_i^0. The average, equilibrium, distribution of mobile ions represents a compromise between these opposing tendencies; corresponding, as usual, to the minimum of the system free energy. Ignoring spatial correlations between the mobile ions (hence the "mean-field" nature of the theory), one could solve the Poisson equation corresponding to the thermally averaged distribution of mobile ions, thus deriving a "thermally averaged" electrostatic potential for the system. Clearly, however, the average ion densities depend on the electrostatic potential through the Boltzmann distribution; namely $n_i(\mathbf{r}) = n_i^0 \exp(-z_i e\Phi(\mathbf{r})/k_BT)$ with e denoting the elementary charge, and z_i the valency of ion species i ($\Phi \equiv 0$ far away from charged surfaces). This "circular" dependence of the electric potential on the local ion densities through Poisson's equation, and the dependence of the latter on the former through Boltzmann's formula, leads to a *self-consistent* relationship which $\Phi(\mathbf{r})$ must fulfill. This relationship is the Poisson-Boltzmann (PB) equation. For a symmetric 1:1 electrolyte solution ($i = \{-1, 1\}$) it is $z_1 = -z_{-1} = 1$, and $n_1^0 = n_{-1}^0 = n_0$. In this case the PB equation reads

$$\frac{\partial^2\Psi}{\partial x^2} + \frac{\partial^2\Psi}{\partial y^2} + \frac{\partial^2\Psi}{\partial z^2} = \frac{1}{l_D^2} \sinh\Psi \tag{2}$$

with $\Psi = e\Phi/k_BT$ denoting the reduced (dimensionless) electrostatic potential and l_D is a (temperature and concentration dependent) constant, known as Debye's *screening length*. This important constant sets the length scale beyond which the Coulombic interaction between two charged particles (or surfaces) is effectively screened by the intervening salt ions. For 1:1 electrolyte solutions at

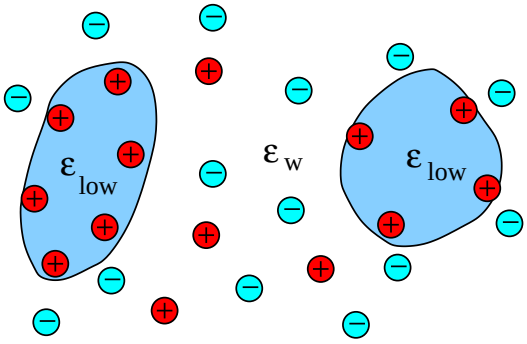

Figure 1. *A common scenario in cellular biology: two macroions of low dielectric constant ε_{low} interact in an aqueous solution (where the dielectric constant is $\varepsilon_w \approx 80$), containing mobile salt ions. Electrostatic interactions between the macroions occur if their respective diffuse counterion layers overlap.*

room temperature, the dependence of the Debye length on the molar concentration of salt is $l_D = 0.304/\sqrt{\mathrm{M}}\ \mathrm{nm}$. Under "physiological" conditions $M \approx 0.1$ and hence $l_D \approx 1\ \mathrm{nm}$.

Writing down the PB equation for multivalent, nonsymmetric or multicomponent salt solutions is straightforward. However, being a nonlinear partial differential equation, analytical solutions of PB equation (even in its symmetric form, Eq. (2)) are available for just a few special cases; see e.g., Ref. [13]. Even numerical solutions usually require advanced computer methods [14]. Yet, it should be noted that once the PB equation is solved one can calculate any desired characteristic of the interacting system. In particular, given the electrostatic potential $\Psi(\mathbf{r})$ is known, we can calculate the local concentrations of mobile ions, $n_{\pm 1} = n_0\ \exp(\mp\Psi)$, around and between the interacting macromolecules. Using these ion densities (or equivalently Ψ) we can also calculate the electrostatic energy, the (counterion) entropy and hence the electrostatic free energy. Following the variation of the free energy as a function of, say, the distance between two macroions, see e.g., Fig. 1, one can derive the solvent-mediated electrostatic interaction between such macromolecules.

The approximate nature of the PB approach is mainly reflected in the neglect of charge-charge correlations [15]. Computer simulations reveal (see e.g., Ref. [16]) that despite its approximate nature, PB theory works well for biopolymers immersed in monovalent salt solutions. Thus, in the following sections all calculations based on PB theory refer to a symmetric, 1:1 electrolyte solution.

3. CATIONIC LIPID-DNA COMPLEXES

In Sec. 1 the complexes formed between DNA and cationic-neutral lipid mixtures were brought up as model system, featuring many of the unique properties characterizing the interaction between lipid membranes and biopolymers. In this section we further elaborate on these systems, emphasizing the ability of the DNA molecules to promote pronounced structural changes of the lipid matrix through strong electrostatic and elastic interactions.

Cationic lipids (CL) are not abundant in living cells. However, recently they have attracted much attention because of their ability to compact DNA by forming the above-mentioned CL-DNA complexes [2], often called *lipoplexes* [17]. Lipoplexes play a central role in current approaches to gene therapy [18], serving as potent transfection vectors, i.e., as carriers of genomic material across the plasma membrane into the cell, on its way to the nucleus. This offers a promising alternative to viral transport vector methods which often suffer from antibody responses. Not yet well understood, however, is how these aggregates enter into living cells, how the DNA molecules dismantle from the cationic lipids, and how do they finally enter the cell nucleus [19,20].

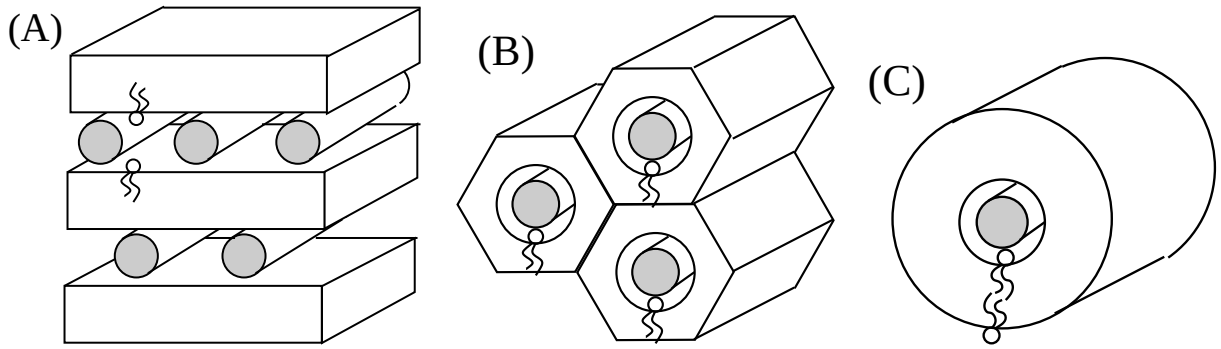

Figure 2. Structural models of CL-DNA complexes. The figure shows, schematically, a two-dimensional cross-section through a plane perpendicular to the DNA (shaded circles). The sandwich-like (L_α^c) structure (A) consists of smectic-like lamellar stacks of charged bilayer in which one-dimensional arrays of DNA strands are intercalated. The honeycomb-like (H_{II}^c) complex (B) is an hexagonally packed bundle of monolayer-coated DNA units. Bilayer-coating of single (or double) stranded DNA leads to the formation of spaghetti-like complexes.

At the very basis of lipoplex formation is simple electrostatics [21]: the negatively charged phosphate groups of DNA attract cationic lipids vesicles. This interaction is strong enough to totally disrupt the vesicles and transform them into compact, often micron-sized, aggregates [22]. Most lipoplex-based transfer vectors use a *mixture* of cationic and neutral lipids [23]. The reason is that by judicious choice of the neutral colipid – also called *helper* lipid – one can significantly enhance the efficiency of DNA transfection as well as reduces the lipoplex toxicity. From a physico-chemical point of view, the helper lipid is helpful in tuning both the charge density of the lipid layers and their curvature elasticity. Commonly used colipids are double-tailed phospholipids, like DOPC or DOPE. While both these lipids are uncharged they exhibit very different structural phase behavior. As already mentioned in Sec. 1, DOPC prefers the lamellar, L_α, phase, whereas DOPE shows a strong tendency for the inverse hexagonal, H_{II}, phase [7]. Cationic lipids, like DOTAP (dioleoyltrimethylammoniumpropane), are generally characterized by very small spontaneous curvatures, and thus self-assemble into planar bilayers.

The choice of different colipids is reflected in the appearance of different lipoplex morphologies, and through this affects the efficiency of gene delivery [24]. With DOPC as the helper lipid the lipoplexes are usually lamellar, (L_α^c). Their "sandwich" structure, as illustrated in Fig. 2, has been determined by X-ray diffraction measurements [4,25] and a variety of complementary methods [22,26–28]. The monolayers of DNA in each gallery of the sandwich complex form a one-dimensional array, characterized by a well defined repeat distance d. For reasons explained below, d depends on lipid composition.

Unlike the lamellar complexes, the structures shown in Fig. 2 B and Fig. 2 C involve highly-bent lipid layers. Fig. 2 B depicts the hexagonal (H_{II}^c), or "honeycomb"-like, complex mentioned in Sec. 1. Its inverse-hexagonal symmetry has unambiguously been confirmed by X-ray diffraction [5,29]. Noting the similarity to the H_{II} phase it is no surprise that the colipid DOPE promotes the formation of the H_{II}^c complex. Note that the repeat unit of the honeycomb-like complex consists of a DNA "rod" wrapped by a lipid monolayer. Like the H_{II} lipid phase, the H_{II}^c complex is stabilized by attractive (hydrophobic) interactions between the lipid chains of neighboring (cylindrically bent) monolayers.

Another possible complex geometry, the "spaghetti"-like structure shown in Fig. 2 C, has been observed in electron microscopy studies [3,30]. As in the H_{II}^c phase this complex consists of a DNA rod wrapped around by a lipid monolayer. However, instead of being surrounded by identical units, the monolayer coated DNA is further surrounded by an oppositely curved, monolayer, giving rise to a bilayer-enveloped DNA complex. Actually, it appears very likely that these complexes are formed upon "direct encounter" between DNA molecules and lipid bilayers, possibly as intermediate structure prior to the formation of H_{II}^c complexes.

The experimental observation and subsequent characterization of the structures shown in Fig. 2 have motivated a number of computer simulations [31,32] and theoretical studies of the structure, stability, and phase behavior of CL-DNA complexes [33–35]. Overall, these studies confirm that the structural and thermodynamic characteristics of these systems indeed reflect a delicate interplay between electrostatic interactions and membrane elasticity. In the following we elaborate on this interplay utilizing the theoretical tools reviewed in Sec. 2.

3.1. Stability of spaghetti-like and honeycomb-like lipoplexes

In both the spaghetti-like and honeycomb-like complexes the negatively charged DNA rods are symmetrically and tightly enveloped by oppositely charged, cationic, lipid monolayers. The concentric geometry of these structures allows, in principle, for exact electrostatic neutralization of the charged phosphate groups on the DNA surface by the cationic lipid charges. When this optimal charge matching condition is fulfilled, the counterions originally bound to the DNA and cationic surfaces are no longer needed for charge neutrality and can thus be released into the bulk solution, thereby increasing their translational entropy. Note, however, that for any given complex radius membrane-DNA charge neutralization requires a very specific cationic/neutral lipid mixture. Although one can experimentally adjust the original lipid mixture, the actual composition in the lipoplex, as well as its radius will be determined by the tendency of the system to minimize its total free energy (see below).

While the concentric DNA-lipid geometry is most favorable on electrostatic

grounds, it generally involves a nonzero elastic deformation energy penalty, resulting from the high ("negative") curvature of the lipid monolayer. This energy penalty may be substantial if the spontaneous curvature of the lipid layer, c_0, is markedly different from its actual curvature in the complex; see Eq. (1). High bending rigidity will also increase the elastic energy penalty. Clearly then, the energetics as well as the detailed structure of the hexagonal-like and spaghetti-like complexes is governed by a delicate balance between the electrostatic and elastic energies.

The interplay between these forces can be understood in terms of a simple model [36], which treats the DNA-monolayer unit as a concentric cylindrical *capacitor*. Its inner surface is that of the DNA, modeled as a rod of fixed radius R^D and surface charge density σ^D. The outer cylinder, of *adjustable* radius R and surface charge density $\sigma = \sigma^D R^D/R$, represents the lipid surface, whose total charge exactly matches the negative DNA charge. The total free energy of the system is then written as a sum of the elastic monolayer energy, as given by Eq. (1) and the charging energy of the capacitor, both of which depend on R. The optimal outer radius is obtained by minimizing the total free energy with respect to R. For lipid mixtures characterized by (the rather typical) spontaneous curvature $c_0 = 0$ one finds the optimal monolayer radius

$$R = \frac{\pi k}{k_B T l_B} l^2 \tag{3}$$

Here $l_B = 7.14$ Å is the Bjerrum length, and $l = 1.7$ Å is the average separation between the charged phosphate groups, measured along the DNA axis. With a typical bending rigidity of $k = 10\ k_B T$ we obtain $R = 12.7$ Å, just slightly larger than the DNA radius $R^D \approx 10$ Å. Clearly, a lower R is impossible, even if k gets much lower. A larger value of k would lead of course to a larger R.

The simple capacitor model embodies several assumptions whose validity deserves further explanation. These assumptions pertain to the following questions:

1. Why should the monolayer seek to adjust its charge density according to $\sigma = \sigma^D R^D/R$, as required by the capacitor model?

2. How is the tendency of certain helper lipids (like DOPE) to form inversely bent structures related to the complex stability?

3. What is the energetic cost associated in protecting the hydrophobic side (of the monolayer enveloping the DNA) from exposure to the aqueous environment?

The first question is related to the tendency of the monolayer-coated DNA to be "*isoelectric*"; namely to ensure that all the negative phosphate charges on the

DNA are exactly neutralized by cationic lipid charges. Charge neutrality of the complex implies that any deviation from isoelectricity must be compensated by transferring mobile counterions from the bulk solution into the confines of the water gap separating the DNA and monolayer surfaces. This process implies a substantial entropy loss of the counterions involved or, equivalently, a highly unfavorable increase of the free energy. In other words, the lipid-DNA complex is of maximal stability at the isoelectric point. Solutions of the PB equation discussed in Sec. 2.2 reveal these conclusions both qualitatively and quantitatively. As noted above the lipid charge density, σ, is regulated by the presence of the colipid. The surface charge density of a monolayer composed of a 1:1 mixture of cationic and colipid is roughly equal to that on the DNA surface.

The answer to the second question is rather clear: a lipid mixture with an intrinsic tendency to form the inverse hexagonal phase (i.e., $c_0 < 0$) will naturally favor the honeycomb and spaghetti-like complexes. Since the spontaneous curvature of cationic lipids is generally small, a simple way to achieve negative spontaneous curvatures is by using helper lipids with this propensity; e.g., DOPE whose most stable aggregation geometry is the inverse hexagonal phase. Tuning the spontaneous curvature of the lipid mixture is, indeed, an important role of the colipid. Detailed phase diagrams demonstrating the richness of lipoplex structures and their variation with lipid composition will be described and analyzed in Sec. 3.3.

Finally, regarding the third question there are two options for the monolayer-coated DNA. That is, the coating of the DNA may involve a whole bilayer instead of only a single monolayer, leading to the spaghetti-like structure shown in Fig. 2 C. Or, alternatively, the monolayer-coated DNA units aggregate into an hexagonally packed array, namely the H_{II}^c complex. Our theoretical investigation suggests the H_{II}^c complex to be generally more stable than the spaghetti-like structure. Still, the latter represents a *metastable* state; it is stable with respect to a spontaneous unwrapping of the DNA-coating bilayer. The formation of the H_{II}^c complex is characterized by a free energy gain of order 1 k_BT per Å length of the DNA [36].

3.2. The sandwich-like, L_α^c-structure

The lamellar (L_α^c) phase of CL-DNA complexes appears if bilayer-forming helper lipids are used. Indeed, lamellar lipoplex structures were detected for mixtures of cationic lipids and neutral lipids with the phosphatidylcholine headgroup [4,25,37]. The DNA strands between the lipid bilayers are parallel to each other, forming a one-dimensional lattice with a correlation length extending over a few DNA strands. The average DNA-to-DNA distance, d, is not fixed but can adjust according to the experimental conditions, namely the lipid-to-DNA charge ratio, ρ, and the bilayer composition, m (ratio of neutral to

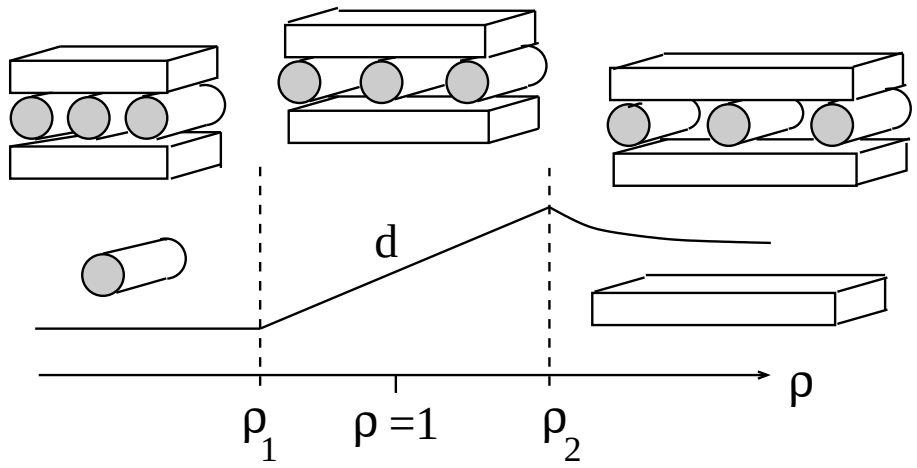

Figure 3. *Schematic illustration of the phase behavior of lamellar CL-DNA self-assembled complexes. Shown is the DNA-to-DNA distance, d, as a function of the lipid-to-DNA charge ratio, ρ. For $\rho < \rho_1$ uncomplexed DNA coexists with L_α^c complexes. For $\rho_1 \leq \rho \leq \rho_2$ the sytem proceeds through a one-phase region where d is proportional to ρ. Note that this region includes the isoelectric point $\rho = 1$ where the fixed charges on the DNA and on the cationic bilayer balance each other. For $\rho > \rho_2$ the L_α^c complexes coexist with excess cationic bilayers. Generally, the composition of the excess bilayer can be different from that in the L_α^c complex.*

cationic lipids). The variations in d with ρ reflect the phase state in which the system resides, as is schematically illustrated in Fig. 3. In particular, for $\rho < \rho_1$ there appears coexistence of sandwich-like complexes with excess DNA. The corresponding DNA-to-DNA distance is small and constant. For intermediate $\rho_1 < \rho < \rho_2$, all lipids and DNA strands are accommodated into the sandwich-like complex. In this, single phase, region d varies linearly with ρ, as implied by the conservation of material. Finally, in the high ρ regime (that is for $\rho > \rho_2$) the sandwich complexes coexist with excess membranes, and the spacing d remains nearly constant. It turns out that the phase boundaries, ρ_1 and ρ_2, depend somewhat on m. But the single phase region, $\rho_1 < \rho < \rho_2$, generally includes the "isoelectric" point, $\rho = 1$, where the fixed negative charges on the DNA balance the same number of positive charges on the cationic lipids. The fact that the single phase region, $\rho_1 < \rho < \rho_2$, is not confined to the point $\rho = 1$ has its origin in the adjustability of the DNA-to-DNA distance d. This additional degree of freedom allows a charge regulation mechanism to take place: for $\rho_1 < \rho < 1$ there are more DNA strands in the complex than would be necessary to neutralize all the lipid charges. The sandwich-like structure then carries a negative excess charge that must be balanced by an appropriate number of positive counterions. Analogously for $1 < \rho < \rho_2$, the L_α^c structure incorporates all lipids, even though this leads to an "overcharging" of the complex.

The experimental observation of the above-described phase behavior raises

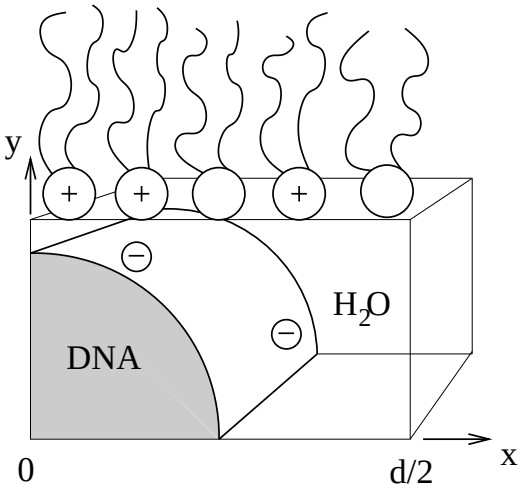

Figure 4. *Schematic representation of the* $\mathrm{L}_\alpha^\mathrm{c}$ *complex. Shown is one-quarter of the unit cell. It is sufficient to solve the PB equation in the aqueous interior. The (dimensionless) electrostatic potential* $\Psi = \Psi(x, y)$ *depends only on the directions,* x *and* y*, parallel and normal to the bilayer. The figure also illustrates the lateral mobility of the lipids. That is, the distribution of the cationic lipids can adjust along the* x*-axis such as to minimize the free energy of the lipoplex.*

a principal question: why do DNA molecules attract each other when being sandwiched between two cationic bilayers? After all, naked DNA does not show attractive forces in monovalent salt solutions. Hence, the formation of one-dimensional DNA arrays between the galleries of the $\mathrm{L}_\alpha^\mathrm{c}$ structure must somehow be mediated by the cationic lipid layers. Indeed, lipid-mediated attractive forces can arise from elastic perturbations induced by membrane-associated macromolecules. In case of DNA, such indirect attractions could compete with the direct electrostatic repulsion between the DNA strands, thus giving rise to an equilibrium distance, d. This mechanism was suggested by Dan [38].

Another, entirely different, scenario is based solely on the electrostatic interactions between the cationic lipid layers and the DNA [39,40]. Here, the $\mathrm{L}_\alpha^\mathrm{c}$ complex adopts its most favorable free energy at the isoelectric point. A corresponding theoretical model that explains the observed phase evolution of the $\mathrm{L}_\alpha^\mathrm{c}$ complex (see Fig. 3) was recently suggested on the basis of PB theory [40] (see also Ref. [39]). To this end, the corresponding nonlinear PB equation was solved within one-quarter of the unit cell of the $\mathrm{L}_\alpha^\mathrm{c}$ structure, as shown in Fig. 4. The individual lipids within the fluid-like bilayers are able to diffuse in lateral direction. Hence, the presence of the DNA can induce a spatial modulation ("polarization") of the lipids along the x-axis, as schematically illustrated in Fig. 4. In fact, the most efficient polarization would lead to a constant electrostatic surface potential on the cationic membranes. However, the tendency of the membrane to become polarized is partially opposed by the loss of entropy, associated with the in-plane demixing of the cationic and neutral lipids. A compromize results where the bilayer does neither keep its surface charge density nor the electrostatic surface potential constant. What is kept constant along the x-axis is the electro-chemical potential of the lipid molecules. This constancy can be taken into account through a special boundary condition of the PB equation. It appears that especially for small compositions, ϕ, of the $\mathrm{L}_\alpha^\mathrm{c}$

complex (where the number of cationic lipids in the bilayer is small) there is a pronounced accumulation of cationic lipids in the vicinity of the DNA. This leads to a more favorable interaction beween the DNA strands and the bilayers, and thus stabilizes the L_α^c complex.

From the numerical solutions of the nonlinear PB equation [40] it appears that the optimal electrostatic free energy is adopted for an isoelectric complex where a maximal number of counterions is released into solution. Notable, maximal release of counterions at the isoelectric point is also found experimentally [41]. At the isoelectric point, the DNA-to-DNA distance is $d^\star = a\phi/l$ where $a = 65$ Å^2 is the cross-sectional area per lipid (which is roughly the same for both lipid species). The existence of a finite d is thus a consequence of isoelectricity, i. e. the tendency to release as many mobile ions as possible into solution. Electrostatics also explains the stability of the L_α^c complexes for deviations from isoelectricity, that is for $\rho_1 < \rho < \rho_2$ and $\rho \neq 1$ where $d \neq d^\star$. Here, the complexes take up either excess DNA (for $\rho_1 < \rho < 1$) or cationic membranes (for $1 < \rho < \rho_2$). Both cases lead to an "overcharging" of the L_α^c complex that is accompanied by an energetic penalty. Yet this is still more favorable than to form an isoelectric complex where excess DNA or excess cationic bilayer would be present that both must shield their charges by immobilizing a diffuse counterion layer. This is the reason why the most stable L_α^c complex, namely the isoelectric one, is in fact unstable with respect to the absorption of either DNA or additional lipids. At $\rho = \rho_1$ or $\rho = \rho_2$ the L_α^c complex becomes unstable. In the former case (at $\rho = \rho_1$) the DNA uptake stops because of the direct DNA-DNA repulsion. In the latter case (at $\rho = \rho_2$) the electrostatic repulsion between neighboring bilayers in the L_α^c complex becomes too large.

Interestingly, the correleations of the DNA strands may extend through the bilayers, giving rise to an intermembrane coupling between the DNA arrays in different galleries of the L_α^c complex. Indeed, for sufficiently low temperatures, where the lipids reside in the gel phase, there is experimental evidence [42] for the formation of a rectangular superlattice of DNA similar to that shown in Fig. 2 A. Even for fluid-like membranes, fingerprint-like patterns in cryo-electron micrographs are indicative of inter-membrane correlations between the DNA arrays [27]. The most reasonable explanation for the appearance of such correlations seems to be a DNA-induced, elastic perturbation of lipid bilayers. This mechanism was analyzed by Schiessel and Aranda-Espinoza [43] on the basis of the linearized PB equation.

3.3. The phase behavior of CL-DNA mixtures

Our discussion of the H_{II}^c and L_α^c structures so far in this section has revealed distict energetic features of each complex type: The H_{II}^c structure benefits from the close proximity between opposite charges of the DNA and cationic

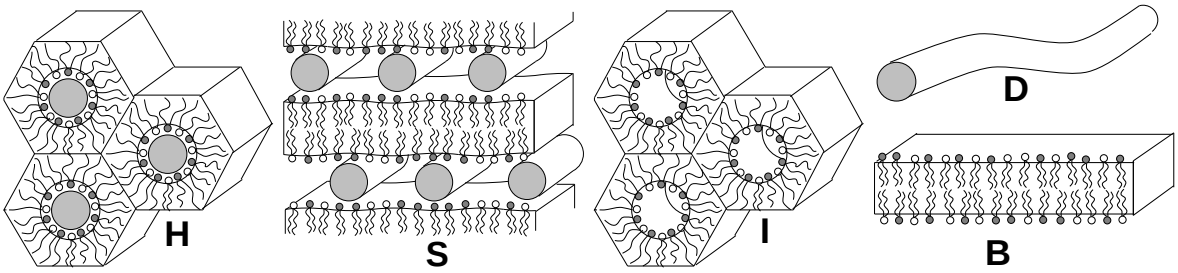

Figure 5. *Schematic illustration of the five macroscopic phases (from Ref. [48], with permission), commonly observed in CL-DNA systems. The phases denoted by H and S are the H^c_{II} and L^c_α complex structures, respectively. The symbols I and B mark the (DNA-free) H_{II} and L_α phases, respectively. D represents uncomplexed DNA. The shaded regions correspond to the DNA cross sectional area. The lipid layers are mixed, consisting of cationic and uncharged (helper) lipids.*

lipids. Yet this electrostatic preference is partially opposed by the elastic energy needed to bend the lipid layers around the DNA strands. On the other hand, the L^c_α complex involves flat membranes that comply with the typical tendency of common cationic lipids to form lamellar phases. In addition to that, the L^c_α structure can adust the DNA-to-DNA distance, d; this extra degree of freedom offers more viability. But here, the geometry of the L^c_α structure implies less perfect electrostatic matching between the DNA and the lipid bilayers. Already these qualitative considerations suggest neither the H^c_{II} complex nor the L^c_α structure to be the ultimate stable complex type. Indeed, recent experiments [5,24,44] evidence the possibility of a transition between the L^c_α and H^c_{II} structure. In fact, there appear two different mechanisms to induce the $L^c_\alpha \rightarrow H^c_{II}$ transition that both lower the energy needed to coat the DNA by a highly bent monolayer. One mechanism employs the colipid as a means to shift the spontaneous curvature, c_0, of the cationic layer [5]. This applies for the common helper lipid DOPE which itself has a preference to assemble into the inverse hexagonal (H_{II}) phase. When used as colipid, DOPE introduces a tendency into the cationic layer to adopt negative curvature, similar to that in the H_{II} phase. The second mechanism is based on a reduction of the elastic energy needed to wrap the cationic layer around DNA. This was achieved experimentaly by the addition of DOPC plus a membrane-soluble cosurfactant (like hexanol) [5]. Here the preference of the cationic layer for the bilayer structure is not affected but the cosurfactant drastically softens the bilayer [45]. This can be understood as a reduction of the bilayer bending rigidity, k (see Eq. (1)), nearly eliminating the energetic penalty needed to bend the cationic lipid layer [46,47].

We shall give a short account of a recent phase calculation that included the

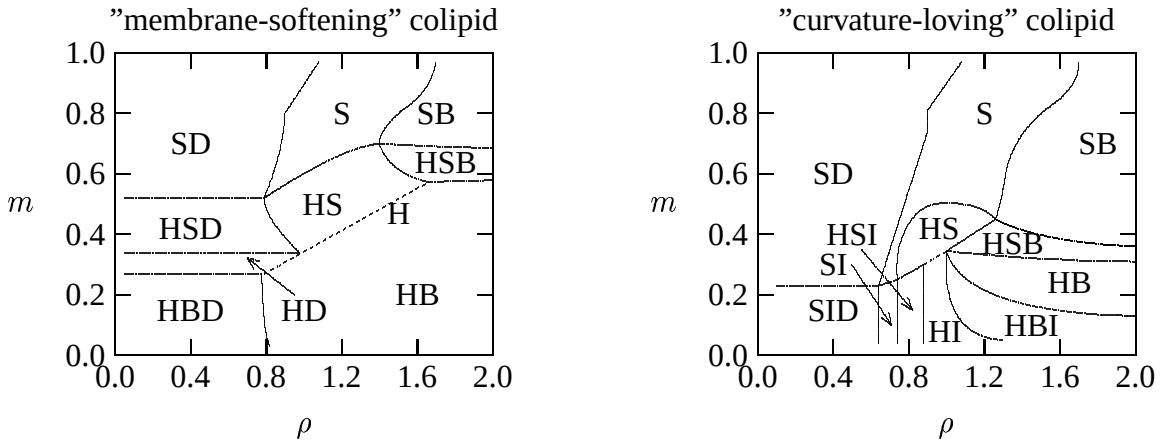

Figure 6. *Calculated phase diagrams of CL-DNA mixtures (from Ref. [48], with permission), as a function of the lipid-to-DNA charge ratio, ρ, and the bilayer composition, m (ratio of neutral to cationic lipids). The left diagram was derived for very soft lipid layers (the actual calculation was carried out for $k = 0.2\ k_BT$ and $c_0 = 0$). This illustrates the effects of adding to the commonly used colipid DOPC a membrane-softening cosurfactant like hexanol. The right diagram models the usage of "curvature-loving" colipids like DOPE. The calculation was performed for a constant bending rigidity $k = 10\ k_BT$ and a spontaneous curvature that changes linearly with the content of colipid from $c_0 = 0$ to $c_0 = -1/25\ \text{Å}^{-1}$. In both diagrams, the straight dashed line marks the single H_{II}^c phase region. The symbols S, B, H and D, denote, respectively, the L_α^c, L_α, H_{II}^c and uncomplexed DNA phases, see Fig. 5.*

appearance of the five structures shown in Fig. 5 [48]. The theoretical tools, sufficient for a detailed model of the phase behavior of CL-DNA mixtures are again PB theory and the quadratic bending energy given in Eq. (1). The spaghetti-like structure was not considered because this complex type does not appear in expriments as a macroscopic phase. Each of the structures in Fig. 5 involves charged surfaces (either the DNA or the cationic lipid layers); the corresponding free energies were calculated using PB theory. The bending energies of the curved lipid layers (concerning structures H and I in Fig. 5) were extracted on the basis of Eq. (1), with linearily composition-dependent spontaneous curvature c_0. The phase calculations were carried out as a function of the lipid-to-DNA charge ratio, ρ, and the bilayer composition, m (ratio of neutral to cationic lipids). For each given values of ρ and m, the actual calculation of the appearing phases involves the minimization of the overall free energy which accounts for all possible combinations of existing phases. The resulting phase diagrams appear rather complex, exhibiting a multitude of phase transitions and coexistences. Yet, the two above-mentioned mechanisms to induce the $L_\alpha^c \rightarrow H_{II}^c$ can be reproduced as shown in Fig. 6. The left diagram in Fig. 6 is derived in the limit of a nearly vanishing bending rigidity of the cationic membrane (in the calculations $k = 0.2\ k_BT$ was used) where the bending of the lipid layers

does not cost an appreciable amount of elastic energy. We have argued above that in this case the H_{II}^c complex is energetically most favorable. This however does not exclude the presence of the L_α^c structure. In fact, Fig. 6 (left diagram) displays regions where the L_α^c complex either coexists with other structures or is even present as a single phase. This is a result of the additional degree of freedom pertaining to the L_α^c complex which allows it to adjust to combinations of ρ and m that do not match the actual need of the H_{II}^c geometry. The pure H_{II}^c phase exists only on a single line in the phase diagram (the broken line in Fig. 6) because it has only one single degree of freedom, namely to adjust its composition. The right diagram in Fig. 6 models the influence of a curvature-loving helper lipid (like DOPE). The calculation was carried out for a constant bending rigidity $k = 10\ k_BT$ and a spontaneous curvature that changes linearly with the content of colipid from $c_0 = 0$ to $c_0 = -1/25\ \text{Å}^{-1}$. This is reflected in the phase diagram by the preferential appearance of the H_{II}^c phase only in the low-m region.

4. ELECTROSTATIC ADSORPTION OF PROTEINS ONTO LIPID MEMBRANES

The adsorption of peripheral proteins onto lipid membranes is frequently driven by electrostatic interactions, and can be characterized by a binding constant that describes the equilibrium between the membrane-bound and free proteins. Determination of the binding constant is one of the main objectives in modeling protein adsorption. There are a number of recent approaches to calculate the adsorption energy of charged proteins onto oppositely charged surfaces, ranging from simple generic models up to atomic-level representations of the protein structures [49–53]. Yet so far, the predictive power of the existing models is still limited. We see three reasons for the current deficiencies: First, the long-range nature of the Coulombic interaction makes exact calculations computationally expansive. A common alternative is the utilization of PB theory which, however, fails if the aqueous solution contains multivalent salt [16,54]. Second, the binding is often influenced by non-electrostatic interactions like the hydrophobic effect [55,56] or conformational changes of the proteins [57]. These effects can be rather specific, depending on the structural details and microscopic interactions of the adsorbing protein. Third, multicomponent lipid bilayers are flexible surfaces and have internal degrees of freedom that affect the adsorption of proteins [58]. That is, unlike a solid surface the lipid membrane actively participates in the adsorption process; the lipid membrane also seems to be a crucial factor for the lateral organization of adsorbing proteins [1,59]. Fig. 7 illustrates two membrane-mediated mechanisms that affect the adsorption energy and interactions between adsorbed proteins. One mechanism involves local curvature modulations of the lipid membrane that enhance the strength of interaction be-

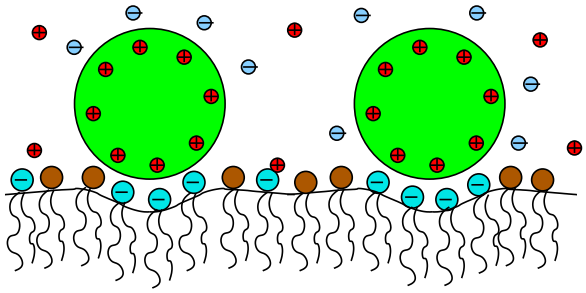

Figure 7. *Mixed lipid membranes are flexible materials with compositional degrees of freedom. They can adapt to the shape and charge density of peripherally adsorbed proteins (illustrated as two large circles). Both the ensuing elastic membrane perturbations and lipid "polarization" effects increase the adsorption strength and give rise to membrane-mediated protein-protein interactions.*

tween the membrane and associated proteins [60,61]. The other one is based on local, protein-induced, demixing of individual membrane components. That is, those membrane lipids that interact more favorably with the adsorbed proteins may migrate towards the protein adsorption sites, replacing the less favorably interacting lipids [62]. In the following we shall focus on the second mechanism.

4.1. Protein-induced lipid demixing

The lateral mobility of the individual lipids in a mixed membrane affects the adsorption energy of proteins. Consider for example a flat, two-component membrane where one lipid species is negatively charged and the other one is electrically neutral. The adsorption of a positively charged protein generally leads to lateral reorganization of the membrane lipids. Negatively charged lipids may accumulate in the vicinity of the protein where they can interact more favorably with the fixed positive charges at the protein surface. This change in the local lipid composition is counteracted by a demixing free energy. One may ask what is the resulting compromise between the two opposing tendencies, and how important is the lateral lipid mobility for the protein adsorption energy?

Let us focus on a recent theoretical investigation that addressed the extent of protein-induced demixing upon the adsorption of a charged protein [63]. The protein was simply modeled as a uniformly charged sphere, and the membrane was kept flat as schematically shown in Fig. 8 (left). PB theory was used to calculate the adsorption free energy of the protein-sphere as function of the adsorption height h. The protein-induced lateral lipid demixing was taken into account by using a special boundary condition for the PB equation which leads to a constant electro-chemical potential of all membrane lipids. In fact, this boundary condition, which reflects the mobility of the charged lipids, is the same as for the calculations of the lamellar CL-DNA complexes (see Sec. 3). The case of constant electro-chemical potential is intermediate between two familiar, limiting, boundary conditions that correspond to either fixed membrane

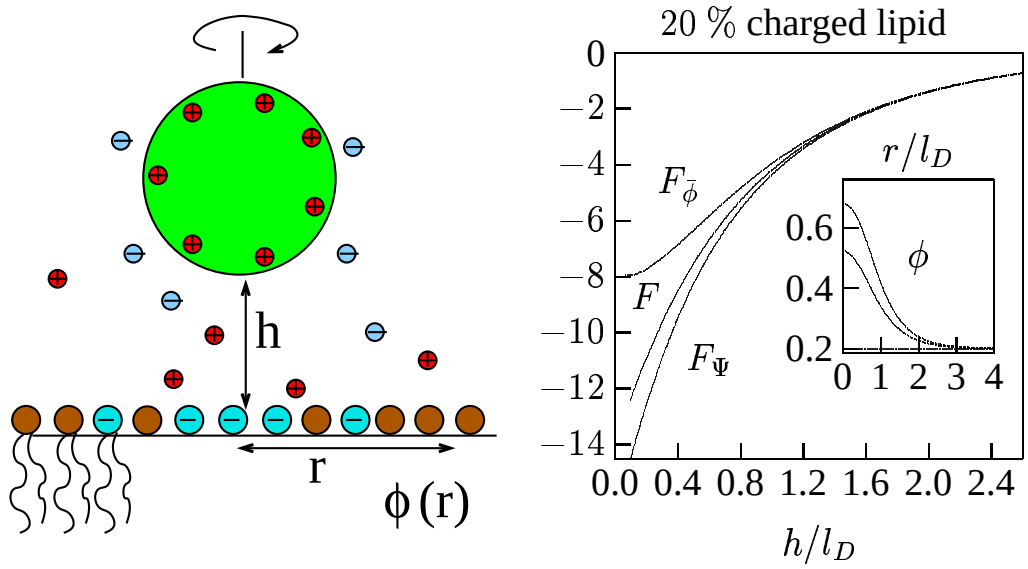

Figure 8. *Left: a uniformly charged sphere adsorbs onto a flat two-component membrane. The individual membrane lipids are mobile; the charged lipid species can optimize its radial composition $\phi(r)$ for any given protein-to-membrane distance h. Right: Predictions from PB theory for the adsorption of a single sphere (of radius $R = 10$ Å with a uniform charge density corresponding to 7 positive charges) onto a mixed membrane that contains 20% negatively charged lipids (from Ref. [63], with permission). The three adsorption free energies (in units of k_BT) correspond to fixed surface charge density ($F_{\bar{\phi}}$), constant electro-chemical potential (F), and constant membrane surface potential (F_Ψ). The inset shows the local membrane composition, ϕ, for the three cases at $h/l_D = 0.3$. The Debye length is $l_D = 10$ Å.*

surface charge density or constant membrane potential. They correspond to two hypothetical limits: infinitely large or vanishingly small in-plane demixing penalty of the lipids. The results of a representative calculation are shown in Fig. 8 (right), corresponding to 20% charged lipids in the membrane, a radius $R = 10$ Å of the protein sphere with 7 positive charges attached to its surface. The three adsorption free energies correspond to fixed surface charge density ($F_{\bar{\phi}}$), constant electro-chemical potential (F), and constant membrane potential (F_Ψ). The inset shows the local membrane composition, ϕ, for the three cases at $h/l_D = 0.3$. Clearly, the binding energy is significantly enhanced if the lipid mobility is taken into account. It turns out that the lipid demixing is particularly important for the biologically most relevant case where highly charged proteins adsorb to weakly charged membranes. The described method was also used to investigate the electrostatic interactions between membrane-adsorbed proteins [63]. These (always repulsive) interactions become relevant if the counterion atmospheres of two proteins start to overlap. Inter-protein repulsion leads to pronounced suppression of the adsorption compared to the simple Langmuir-like adsorption where protein-protein repulsion is not taken into account.

The situation becomes more involved if additional short-range attractions are present between individual lipids of the same type. This generally introduces a tendency of the lipids for macroscopic phase separation. However, this tendency can easily be counterbalanced by the electrostatic repulsion acting between charged lipids. This opens an interesting possibility: positively charged proteins that adsorb onto the membrane would effectively neutralize the negative lipid charges. The repulsive part of the interactions between the charged lipids would disappear and, consequently, the tendency for macroscopic phase separation reappears. Indeed, simple electrostatic models that are based on PB theory predict the ability of protein adsorption-induced phase separation [64,65]. The existence of membrane domains has recently received much attention [64,66–68]. Hence, it would be interesting to further develop microscopic models that describe biopolymer-induces phase separations in lipid membranes.

5. MEMBRANE REORGANIZATION INDUCED BY INTEGRAL PROTEINS

A considerable fraction of all proteins is sealed into the lipid bilayer by hydrophobic interactions. Nearly all integral proteins span entirely the lipid bilayer. What varies is the number and secondary structure of the membrane-spanning segments. Yet, despite the structural and functional variety of transmembrane proteins there is a distinct difference to the host bilayer: transmembrane protein segments are much more rigid than the surrounding lipid phase [69]. Thus, the strong hydrophobic forces that anchor the protein into the membrane create an interface between a rigid membrane inclusion and the fluid-like membranous environment. Note that this is an entirely non-specific effect which is present for all protein-containing membranes; its consequences are evidenced experimentally for many different systems. The focus in this section is on our own recent efforts to model non-specific interactions between integral proteins and lipid membranes.

There is an immediate consequence of the different rigidities between integral proteins and membranes: The membrane must adjust to the prescribed shape and size of the protein (and not vice versa). For example, if the length, $2h_P$, of the hydrophobic span of an integral protein differs from the hydrophobic thickness, $2h_0$, of the host bilayer, then there will be an elastic deformation of the bilayer so as to *locally* match the protein size. The mismatch between h_P and h_0 is generally referred to as *hydrophobic mismatch* which can be positive or negative as schematically shown in Fig. 9. Even though the hydrophobic mismatch is usually quite small (a few Å) its consequences can be observed by appropriate experiments (for a recent summary see Killian [6]). With regard to the lipids there is an increase in chain order close to integral proteins [70], there are shifts in the main phase transition temperature, and there is a lipid sorting

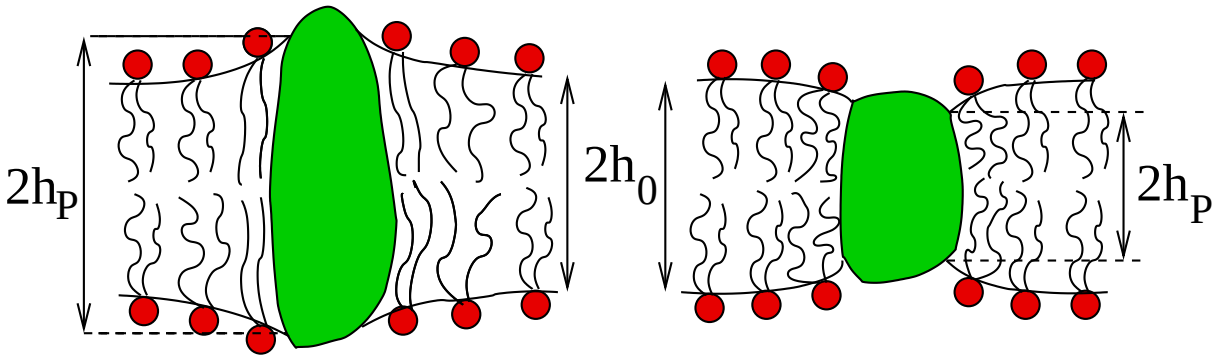

Figure 9. *Schematic illustration of positive (left) and negative (right) hydrophobic mismatch. The length of the hydrophobic span of the protein is denoted by* $2h_P$*. The hydrophobic thickness of the membrane far away from the protein in* $2h_0$*.*

mechanism for mixed membranes [71]. Perhaps most exiting however, integral proteins can mediate structural phase transitions of bilayers as will be discussed below. Also the protein itself can be affected through hydrophobic mismatch in various ways . Experimental evidence exists for modifications in protein activity and conformation, for mismatch-induced protein aggregation, for a tilt of the membrane spanning segments, and for protein delocalization on the membrane surface [6,72,73].

Most of the theoretical efforts in the past have focused on the lateral organization of membrane proteins [1]. The key here is to understand how the membrane mediates interactions between integral proteins in membranes. In the following we shall discuss our own theoretical investigations to model lipid-protein interactions using a microscopic molecular-level model and a phenomenological approach.

5.1. Predictions for lipid-protein interaction from microscopic models

On a microscopic scale, the presence of an integral protein perturbs the packing of the neighboring lipids. Such a perturbation is present even if there is no hydrophobic mismatch between the protein and membrane. Generally, membrane perturbations may arise from specific interactions between the lipid chains and the amino acid residues of the transmembrane protein segments. Another, non-specific, mechanism is the loss of conformational freedom experienced by the lipid chains in the vicinity of a rigid protein surface. This effect was recently investigated on the basis of molecular-level, mean-field, chain packing theory for a single (and sufficiently large) protein with given hydrophobic mismatch [74]. Our objective was to investigate the implications of the conformational chain restrictions on the interactions between integral membrane proteins [75]. To this end, two interacting (and sufficiently large) integral pro-

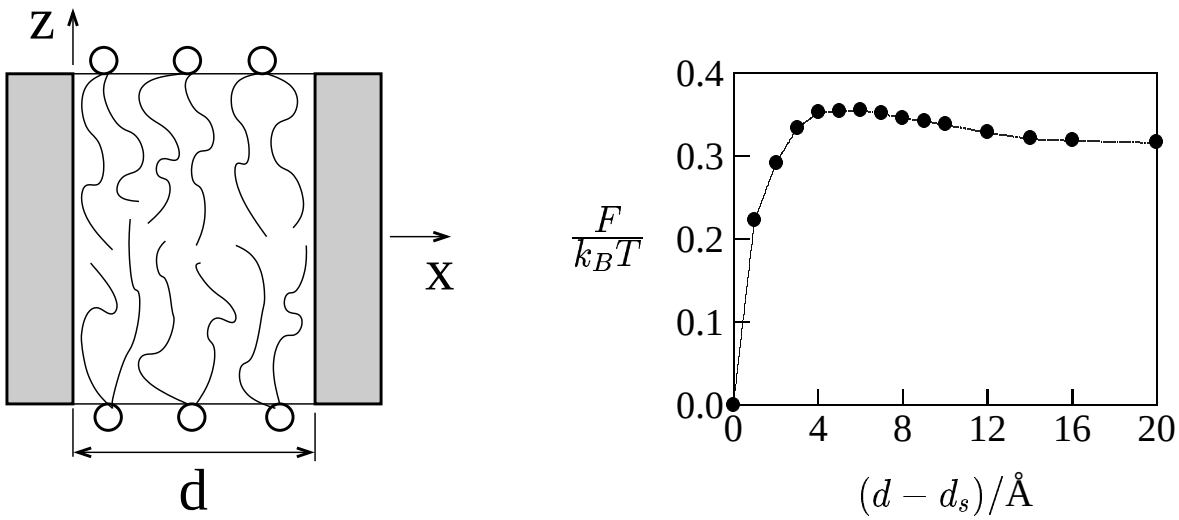

Figure 10. *Left: schematic illustration of a lipid membrane bounded by two rigid, impenetrable, walls. The distance between the walls is d. According to chain packing theory, the probability distributions for all accessible lipid chain conformations inside the bilayer are calculated so as to achieve uniform density of chain segments everywhere within the hydrocarbon core. Right: The wall-induced perturbation free energy (per monolayer and per unit length $L = 1$ Å of the walls) as a function of the wall-to-wall separation $d - d_s$ (where d_s is a constant on the order of the cross-sectional extension of a single lipid chain).*

teins were represented by two rigid walls that are perpendicularly embedded in a symmetric lipid bilayer as shown schematically in Fig. 10 (left). The conformational chain properties were calculated on the basis of the above-mentioned chain packing theory. The key point in this approach [76,77] is the assumption of uniform density of lipid chain segments everywhere within the hydrocarbon core. This is achieved by an appropriate statistical behavior of the flexible lipid chains. In an unperturbed membrane, the average statistical behavior is the same for all lipids. Not so in the presence of the rigid protein-walls. Here, different lipid chains have different conformational space available. The most restricted lipid chains are those in immediate neighborhood to either one of the walls. More generally, the average conformational behavior of the lipid chains depends on the distance to the walls. If the walls are sufficiently close to each other, a given chain can be influenced by both walls. This gives rise to short-range interactions between the walls. The prediction of the chain-packing theory for the interaction potential between walls of distance d is shown in Fig. 10 (right). Most notably, the potential is non-monotonic, exhibiting a maximum at some intermediate wall-to-wall distance. The appearance of a maximum can be understood in terms of a simple *director model* in which each lipid chain is represented as a fluctuating director [75].

Non-monotonic interaction potentials are also found using other micro-

scopic models to study membrane-mediated protein-protein interactions. Recent Monte-Carlo simulations of a coarse-grained membrane model [78,79] revealed a rather complex interaction potential between rigid membrane inclusions: short and long-range attraction was separated by a repulsive barrier for distances between the inclusions somewhat larger than the lipid diameter. Similarly, a recent approach based on hypernetted chain integral equation formalism [80] (where the lateral density-density response function of the hydrophobic core was extracted from a molecular dynamics simulation [81]) also resulted in an energetic barrier upon the approach of two integral proteins.

5.2. Membrane elasticity theory

Membrane elasticity theory treats the bilayer as an elastic continuum. The membrane free energy is expressed with respect to a certain (and usually small) number of *order parameters* where each order parameter represents a degree of freedom of the system. The interaction of a rigid biopolymer with the membrane imposes a localized perturbation of some lipid molecules. This perturbation induces an elastic response of the bilayer; the response and the corresponding membrane free energy can be calculated in terms of elastic moduli through which the material properties of the membrane are characterized. In the past, membrane elasticity theory was frequently used to model interactions between bilayers and integral proteins. Two different cases appear depending on whether an integral protein is symmetric or asymmetric [82]. Symmetric ones leave the midplane of a bilayer planar (unless, of course, the bilayer itself is asymmetric) and cause exponentially decaying perturbations and interactions. In contrast, interactions between asymmetric proteins are long-ranged [83,84].

The most significant experimental motivation to apply membrane elasticity theory comes from studies of interactions between model membranes and gramicidin A [85]. This miniprotein consists of two monomers that dimerize in a bilayer to form a (symmetric) cation-selective channel. The average channel lifetime depends on the properties of the host membrane [86–88]; via monitoring its lifetime, the channel can be used as a force transducer that reflects the energetics of a lipid bilayer. Let us give a basic introduction into the theory for symmetric proteins (like gramicidin A). To this end, it is sufficient to describe, say, the upper monolayer by the local (effective) thickness, h, of the lipid chain region or, equivalently, the relative thickness dilation $u = h/h_0 - 1$. In the most simple case, two modes of deformation are taken into account in the free energy of a perturbed bilayer. Then, F can be written as

$$F = \int_A da \left[\frac{K}{2} u^2 + \frac{k}{2} (c_1 + c_2 - c_0)^2 \right] \tag{4}$$

The first term in Eq. (4) is due to the stretching (or compression) of the lipid chains; K is the corresponding stretching modulus of a lipid monolayer. The

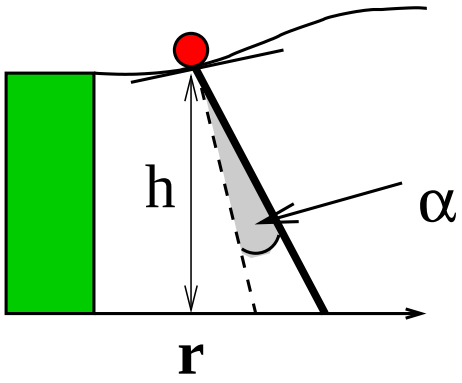

Figure 11. *Schematic illustration of the lipid tilt degree of freedom. Generally, lipid tilt refers to the angle, α, of the average lipid chain director (thick line) at position $\mathbf{r} = \{x, y\}$ of the head group (circle), measured with respect to the normal direction (broken line) of the hydrocarbon-water interface. Another, commonly used, order parameter is the local hydrophobic thickness dilation, $u = h/h_0 - 1$.*

second term in Eq. (4) is equivalent to the first term in Eq. (1), and accounts for the splay energy of the lipid molecules. To a good approximation the principal curvatures c_1 and c_2 can be measured at the hydrocarbon chain-water interface. Realizing that $c_1 + c_2 \approx h_0(\partial^2 u/\partial x^2 + \partial^2 u/\partial y^2)$ we find F to be a function of a single order parameter, namely $u(x, y)$ where the x, y-plane coincides with the bilayer midplane. Minimization of F then requires to solve an appropriate Euler equation for which the proteins enter as boundary conditions. For example, in case of a given hydrophobic mismatch the Euler equation must be solved such that at the protein boundaries we find $u(x, y) = (h_p/h_0 - 1)$.

Already the simple approach according to Eq. (4) seems to well describe real membranes. In fact, the predictions of membrane elasticity theory according to Eq. (4) agree with experimental results. This concerns the so-called spring constant [89] that describes the energetic response of a bilayer membrane to a given, gramicidin A-imposed, hydrophobic mismatch [90]. It also appears to reproduce well the experimental findings of gramicidin A-induced membrane thinning [91]. Note that a number of previous theoretical investigations have basically used Eq. (4) to calculate lipid-protein [92,93] and membrane-mediated protein-protein interactions [94,95].

Recently, it was suggested that another elastic mode of deformation should be taken into account when applying membrane elasticity theory to structurally perturbed membranes, namely the ability of the lipid chains to tilt with respect to the hydrocarbon chain-water interface [96–102] as schematically illustrated in Fig. 11. Lipid tilt is possible despite the fact that the membrane is in the fluid-like state. In fact, here the tilt refers to the *average* orientation of the flexible chains. The ability to tilt gives rise to a second order parameter, the tilt angle α (besides u), which generally lowers the free energy, F, and facilitates the spatial relaxation of the membrane. With the possibility of a local tilt angle α the free energy becomes

$$F = \int_A da \left[\frac{K}{2} u^2 + \frac{k}{2} (\tilde{c}_1 + \tilde{c}_2 - c_0)^2 + \frac{k_t}{2} \alpha^2 \right] \tag{5}$$

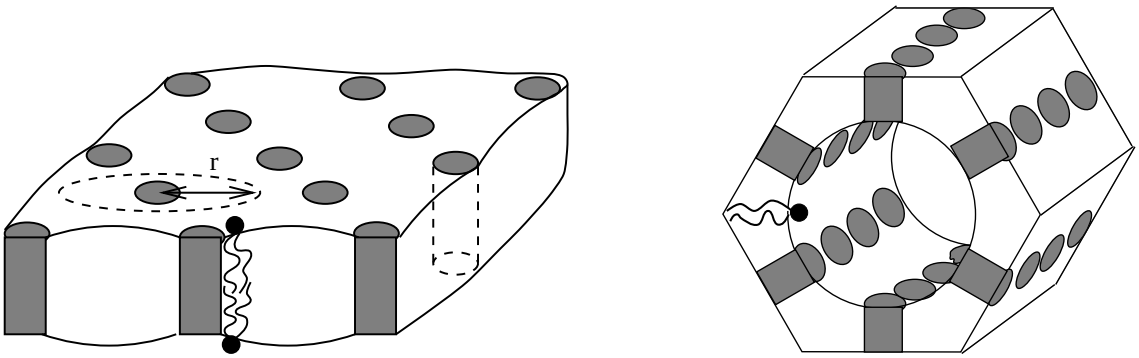

Figure 12. The structures of the inclusion-containing L_α (left) and H_{II} phases (right), the latter one as suggested by Killian [104]. The shaded regions represent the peptide locations (from Ref. [101], with permission).

where k_t is the tilt modulus which was very roughly estimated to be on the order of $k_t \approx 0.1\, k_B T/\text{Å}^2$ [99]. The quantities $\tilde{c}_1$ and $\tilde{c}_2$ account for the splay of the monolayer. For $\alpha = 0$ the splay $\tilde{c}_1 + \tilde{c}_2$ becomes equal to the sum of the principal curvatures $c_1 + c_2$ of the chain-water interface. But generally, lipid splay can also arise through changes in the tilt angle α as was recently analyzed by Hamm and Kozlov [100]. The lipid tilt degree of freedom gives rise to new interesting phenomena, like a "ripple" instability of a pure membrane [97], or the formation of sharp membrane edges [103]. It also opens new ways to model structurally perturbed lipid phases like the inverse-hexagonal (H_{II}) phase [101,99].

5.3. Protein-induced structural phase transitions of lipid membranes

Aside from the effects on the lateral organization of planar lipid bilayers, integral proteins are able to affect the structural phase behavior of membranes. This was shown for gramicidin A and a number of synthetic α-helical transmembrane peptides residing in common lipid membranes [104–106]. In fact, these peptides are able to induce the $L_\alpha \rightarrow H_{II}$ transition in membranes that without the peptide have a strong tendency to self-assemble into planar bilayers. It was found that the $L_\alpha \rightarrow H_{II}$ transition could be induced above a critical concentration of the peptide in the membrane. Moreover, the transition only takes place for a sufficiently large *negative* hydrophobic mismatch, and only if the peptides contain interface-anchored tryptophans (probably to prevent peptide aggregation in the membrane). A structural model suggested by Killian et al [104] for the arrangement of the peptides in both the L_α and H_{II} phases is shown in Fig. 12. According to this model, the peptides in the H_{II} phase are arranged in such a way that they span the entire hydrophobic region between neighboring tubes.

We have recently presented a theoretical investigation of the peptide-

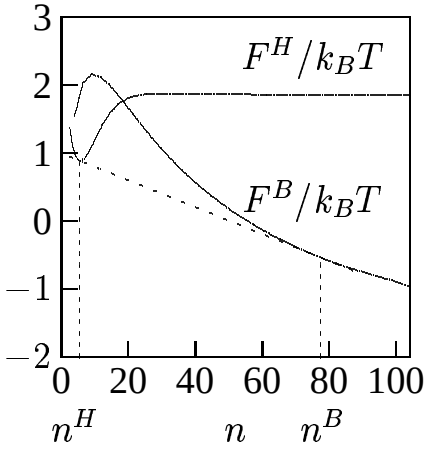

Figure 13. The free energy per inclusion in the inverse hexagonal phase (F^H), and in the bilayer phase (F^B), as a function of the number of lipids per inclusion, n. The dotted lines characterize the 'common tangent', and the coexistence values of n^B and n^H. The results shown correspond to lipid layers with $c_0 = 0$, containing cylindrical inclusions with 35% negative hydrophobic mismatch (adapted from Ref. [101]).

induced $L_\alpha \rightarrow H_{II}$ transition [101]. It was based on membrane elasticity theory applied to the peptide-containing L_α and H_{II} phases. As is common in membrane elasticity theory, the peptides were represented as rigid inclusions of given shape and size. A significant feature of our investigation was the usage of a molecular-level model that accounts for the principal forces governing the structural phase behavior of lipid molecules, namely head group repulsion (f_{hg}), tail repulsion (f_c), and the interfacial tension (f_i) between the hydrocarbon-water interface. In fact, the resulting free energy per lipid, $f = f_{hg} + f_c + f_i$, can be used to calculate the elastic properties of a lipid layer. The lipid tilt degree of freedom appears naturally in this approach, and all the elastic constants defined in Eq. (5) can be calculated in terms of the molecular model. Hence, our model of the inclusion-containing L_α and H_{II} phases is based on Eq. (5) and an appropriate minimization of the free energies, F^B and F^H, for the bilayer and the inverse hexagonal phase, respectively. Once F^B and F^H are calculated as a function of the peptide concentration, the coexisting phases can by derived from common thermodynamic equilibrium conditions. In the present case, this is equivalent to finding the common tangent of F^B and F^H as shown in Fig. 13. In agreement with experimental results we found that only sufficiently short peptides are able to drive the $L_\alpha \rightarrow H_{II}$ transition, once the peptide concentration exceeds a critical value. In the coexisting bilayer the peptide concentration is much smaller than in the H_{II} phase (see Fig. 13).

6. CONCLUSIONS AND OUTLOOK

Lipid membranes are complex fluids that adapt their structure and conformation to various kinds of associated biopolymers. This ability gives rise to exciting phenomena, ranging from lateral modulations of membrane structure to morphological phase transitions. Our understanding is challenged because membrane-biopolymer interactions are ultimately relevant in biology and biotechnology. The present chapter focuses entirely on elastic and electrostatic

interactions which is only a fraction of what is present in real systems. However, it appears that already these two types of interaction are sufficient to principally understand a number of experimental observations, like the formation of CL-DNA complexes or protein induced structural phase transitions of lipid membranes.

Note that this chapter does not deal with partially membrane penetrating biopolymers, like amphipathic peptides. Even though there are intensive experimental activities to understand the action of amphipathic, membrane-active, peptides on lipid bilayers [107–109], there are only a few theoretical investigations [110,111] and computer simulations performed so far. One reason for our current deficiencies in modeling the association between amphipathic peptides and lipid bilayers is perhaps the profound coupling between electrostatic and elastic interactions: amphipathic peptides insert partially into membranes and cause substantial perturbations of the hydrophobic core. At the same time, most of these peptides are highly charged which influences their mutual interactions. Hence, cooperative behavior, like peptide-induced formation of membrane pores can be expected to sensitively depend on the interplay between electrostatic and elastic interactions. Further work is required to better understand these important systems.

ACKNOWLEDGMENTS

We would like to thank our collaborators and co-workers, in particular D. Harries, W. M. Gelbart, M. M. Kozlov, and A. Ulrich. We apologize to all colleagues who work on lipid-biopolymer interaction but are not directly referenced. SM is generously supported by TMWFK.

REFERENCES

[1] T. Gil, J. H. Ipsen, O. G. Mouritsen, M. C. Sabra, M. M. Sperotto and M. J. Zuckermann, Biophys. Biochim. Acta., 1376 (1998), 245.
[2] C. R. Safinya, Curr. Opin. Struct. Biol., 11 (2001), 440.
[3] B. Sternberg, F. L. Sorgi and L. Huang, FEBS Letters, 356 (1994), 361.
[4] J. O. Rädler, I. Koltover, T. Salditt and C. R. Safinya, Science, 275 (1997), 810.
[5] I. Koltover, T. Salditt, J. O. Rädler and C. R. Safinya, Science, 281 (1998), 78.
[6] J. A. Killian, Biophys. Biochim. Acta., 1376 (1998), 401.
[7] J. M. Seddon and R. H. Templer, in Structure and Dynamics of Membranes, (eds.) R. Lipowsky and E. Sackmann, vol. 1, Elsevier, Amsterdam, 1995, second edn. 98–160.

[8] J. N. Israelachvili, Intermolecular and Surface Forces, Academic Press, 1992, second edn.
[9] D. F. Evans and H. Wennerström, The colloidal domain, where physics, chemistry, and biology meet, VCH publishers, 1994, second edn.
[10] W. Helfrich, Z. Naturforsch., 28 (1973), 693.
[11] D. P. Tieleman, S. J. Marrink and H. J. C. Berendsen, Biophys. Biochim. Acta., 1331 (1997), 235.
[12] E. J. W. Verwey and J. T. G. Overbeek, Theory of the stability of lyophobic colloids, Elsevier, Elsevier, New York, 1948.
[13] D. Andelman, in Structure and Dynamics of Membranes, (eds.) R. Lipowsky and E. Sackmann, vol. 1, Elsevier, Amsterdam, 1995, second edn. 603–642.
[14] W. Rocchia, E. Alexov and B. Honig, J. Phys. Chem. B, 105 (2001), 6507.
[15] V. Vlachy, Annu. Rev. Phys. Chem, 50 (1999), 145.
[16] H. Wennerström, B. Jönsson and P. Linse, J. Chem. Phys, 76 (1982), 4665.
[17] P. L. Felgner, T. R. Gadek, M. Holm, R. Roman, H. W. Chan, M. Wenz, J. P. Northrop, G. M. Ringold and M. Danielsen, Proc. Natl. Acad. Sci. U.S.A., 84 (1987), 7413.
[18] P. L. Felgner, Scientific American, 276 (1997), 102.
[19] M. J. Hope, B. Mui, S. Ansell and Q. F. Ahkong, Molecular Membrane Biology, 15 (1998), 1.
[20] Y. Xu and F. C. Szoka Jr., Biochemistry, 35 (1996), 5616.
[21] W. M. Gelbart, R. Bruinsma, P. A. Pincus and V. A. Parsegian, Physics today, 53 (2000), 38.
[22] S. Hübner, B. J. Battersby, R. Grimm and G. Cevc, Biophys. J., 76 (1999), 3158.
[23] S. W. Hui, M. Langner, Y.-L. Zhao, R. Patrick, E. Hurley and K. Chan, Biophys. J., 71 (1996), 590.
[24] J. Smisterova, A. Wagenaar, M. C. Stuart, E. Polushkin, G. ten Brinke, R. Hulst and J. B. E. D. Hoekstra, J. Biol. Chem, 276 (2001), 47615.
[25] D. D. Lasic, H. Strey, M. C. A. Stuart, R. Podgornik and P. M. Frederik, J. Am. Chem. Soc., 119 (1997), 832.
[26] Y. S. Tarahovsky, R. S. Khusainova, A. V. Gorelov, T. I. Nicolaeva, A. A. Deev, A. K. Dawson and G. R. Ivanitsky, FEBS Letters, 390 (1996), 133.
[27] B. J. Battersby, R. Grimm, S. Hübner and G. Cevc, Biophys. Biochim. Acta., 1372 (1998), 379.
[28] B. Pitard, O. Aguerre, M. Airiau, A. M. Lachages, T. Boukhnikachvili, G. Byk, C. Dubertret, C. Herviou, D. Scherman, J. F. Mayaux and J. Crouzet, Proc. Natl. Acaf. Sci. USA, 94 (1997), 14412.
[29] T. Boukhnikachvili, O. AguerreChariol, M. Airiau, S. Lesieur, M. Ollivon

and J. Vacus, FEBS Letters, 409 (1997), 188.
[30] B. Sternberg, J. Liposome Res., 6 (1996), 515.
[31] D. A. Pink, B. Quinn, J. Moeller and R. Merkel, Phys. Chem. Chem. Phys., 2 (2000), 4529.
[32] S. Bandyopadhyay, M. Tarek and M. L. Klein, J. Phys. Chem. B, 103 (1999), 10075.
[33] L. Golubovic and M. Golubovic, Phys. Rev. Lett., 80 (1998), 4341.
[34] C. S. O'Hern and T. C. Lubensky, Phys. Rev. Lett., 80 (1998), 4345.
[35] C. Fleck, R. R. Netz and H. H. von Grünberg, Biophys. J., 82 (2002), 76.
[36] S. May and A. Ben-Shaul, Biophys. J., 73 (1997), 2427.
[37] N. S. Templeton, D. D. Lasic, P. M. Frederik, H. H. Strey, D. D. Roberts and G. N. Pavlakis, Nature Biotechnology, 15 (1997), 647.
[38] N. Dan, Biophys. J., 73 (1997), 1842.
[39] R. Bruinsma, Eur. Phys. J. B, 4 (1998), 75.
[40] D. Harries, S. May, W. M. Gelbart and A. Ben-Shaul, Biophys. J., 75 (1998), 159.
[41] K. Wagner, D. Harries, S. May, V. Kahl, J. O. Rädler and A. Ben-Shaul, Langmuir, 16 (2000), 303.
[42] F. Artzner, R. Zantl, G. Rapp and J. Rädler, Phys. Rev. Lett., 81 (1998), 5015.
[43] H. Schiessel and H. Aranda-Espinoza, Eur. Phys. J. E, 5 (2001), 499.
[44] D. Simberg, D. Danino, Y. Talmon, A. Minsky, M. E. Ferrari, C. J. Wheeler and Y. Barenholz, J. Biol. Chem., 276 (2001), 47453.
[45] C. R. Safinya, E. B. Sirota, D. Roux and G. S. Smith, Phys. Rev. Lett., 62 (1989), 1134.
[46] I. Szleifer, D. Kramer, A. Ben-Shaul, W. M. Gelbart and S. A. Safran, J. Chem. Phys., 92 (1990), 6800.
[47] S. May and A. Ben-Shaul, J. Chem. Phys., 103 (1995), 3839.
[48] S. May, D. Harries and A. Ben-Shaul, Biophys. J., 78 (2000), 1681.
[49] P. Warszyńsky and Z. Adamczyk, J. Colloid Interface Sci, 187 (1997), 283.
[50] S. A. Palkar and A. M. Lenhoff, J. Colloid Interface Sci, 165 (1994), 177.
[51] D. McCormack, S. L. Carnie and D. Y. C. Chan, J. Colloid Interface Sci, 169 (1995), 177.
[52] N. Ben-Tal, B. Honig, R. M. Peitzsch, G. Denisov and S. McLaughlin, Biophys. J., 71 (1996), 561.
[53] N. Ben-Tal, B. Honig, C. Miller and S. McLaughlin, Biophys. J., 73 (1997), 1717.
[54] N. Gronbech-Jensen, R. J. Mashl, R. F. Bruinsma and W. M. Gelbart, Phys. Rev. Lett., 78 (1999), 2477.
[55] S. McLaughlin and A. Aderem, Trends in Biochem. Sci., 20 (1995), 272.

[56] S. H. White and W. C. Wimley, Biophys. Biochim. Acta., 1376 (1998), 339.
[57] S. H. White and W. C. Wimley, Annu. Rev. Biophys. Biomol. Struct., 28 (1999), 319.
[58] A. Ben-Shaul, N. Ben-Tal and B. Honig, Biophys. J., 71 (1996), 130.
[59] P. Schiller and H. J. Mögel, Phys. Chem. Chem. Phys., 2 (2000), 4563.
[60] H. Schiessel, Eur. Phys. J. B, 6 (1998), 373.
[61] P. Schiller, Mol. Phys., 98 (2000), 493.
[62] T. Heimburg, B. Angerstein and D. Marsh, Biophys. J., 76 (1999), 2575.
[63] S. May, D. Harries and A. Ben-Shaul, Biophys. J., 79 (2000), 1747.
[64] G. Denisov, S. Wanaski, P. Luan, M. Glaser and S. McLaughlin, Biophys. J., 74 (1998), 731.
[65] D. Harries, S. May and A. Ben-Shaul, Colloids and Interfaces A, 208 (2002), 41.
[66] D. A. Brown and E. London, J. Mem. Biol., 164 (1998), 103.
[67] A. J. Bradley, E. Maurer-Spurej, D. E. Brooks and D. V. Devine, Biochemistry, 38 (1999), 8112.
[68] A. K. Hinderliter, P. F. F. Almeida, C. E. Creutz and R. L. Biltonen, Biochemistry, 40 (2001), 4181.
[69] K. Gekko and H. Noguchi, J. Phys. Chem., 83 (1979), 2706.
[70] M. R. R. de Planque, D. V. Greathouse, R. E. Koeppe, H. Schäfer, D. Marsh and J. A. Killian, Biochemistry, 37 (1998), 9333.
[71] F. Dumas, M. M. Sperotto, M. C. Lebrun, J. F. Tocanne and O. G. Mouritsen, Biophys. J., 73 (1997), 1940.
[72] M. R. R. de Planque, E. Goormaghtigh, D. V. Greathouse, R. E. Koeppe, J. A. W. Kruijtzer, R. M. J. Liskamp, B. de Kruijff and J. A. Killian, Biochemistry, 40 (2001), 5000.
[73] B. Bechinger, FEBS Letters, 504 (2001), 161.
[74] D. R. Fattal and A. Ben-Shaul, Biophys. J., 65 (1993), 1795.
[75] S. May and A. Ben-Shaul, Phys. Chem. Chem. Phys., 2 (2000), 4494.
[76] A. Ben-Shaul and W. M. Gelbart, in Micelles, Membranes, Microemulsions, and Monolayers, (eds.) W. M. Gelbart, A. Ben-Shaul and D. Roux, Springer, New York, 1994, first edn. 359–402.
[77] A. Ben-Shaul, in Structure and Dynamics of Membranes, (eds.) R. Lipowsky and E. Sackmann, vol. 1, Elsevier, Amsterdam, 1995 359–402.
[78] T. Sintes and A. Baumgärtner, J. Phys. Chem. B, 102 (1998), 7050.
[79] T. Sintes and A. Baumgärtner, Physica A, 249 (1998), 571.
[80] P. Lagüe, M. J. Zuckermann and B. Roux, Biophys. J., 79 (2000), 2867.
[81] S. E. Feller, R. M. Venable and R. W. Pastor, Langmuir, 13 (1997), 6555.
[82] S. May, Curr. Op. Coll. Int. Sci., 5 (2000), 244.

[83] M. Goulian, R. Bruinsma and P. Pincus, Europhys. Lett., 22 (1993), 145.
[84] K. S. Kim, J. Neu and G. Oster, Biophys. J., 75 (1998), 2274.
[85] T. A. Harroun, W. T. Heller, T. M. Weiss, L. Yang and H. W. Huang, Biophys. J., 76 (1999), 937.
[86] J. A. Lundbæk, A. M. Maer and O. S. Andersen, Biochemistry, 36 (1997), 5695.
[87] J. A. Lundbæk, P. Birn, J. Girshman, A. J. Hansen and O. S. Andersen, Biochemistry, 35 (1996), 3825.
[88] J. A. Lundbæk and O. S. Andersen, J. Gen. Physiol., 104 (1994), 645.
[89] C. Nielsen, M. Goulian and O. S. Andersen, Biophys. J., 74 (1998), 1966.
[90] J. A. Lundbæk and O. S. Andersen, Biophys.J, 76 (1999), 889.
[91] T. A. Harroun, W. T. Heller, T. M. Weiss, L. Yang and H. W. Huang, Biophys. J., 76 (1999), 3176.
[92] N. Dan and S. A. Safran, Biophys. J., 75 (1998), 1410.
[93] C. Nielsen and O. S. Andersen, Biophys. J., 79 (2000), 2583.
[94] N. Dan, P. Pincus and S. A. Safran, Langmuir, 9 (1993), 2768.
[95] H. Aranda-Espinoza, A. Berman, N. Dan, P. Pincus and S. A. Safran, Biophys. J., 71 (1996), 648.
[96] F. C. MacKintosh and T. C. Lubensky, Phys. Rev. Lett., 67 (1991), 1169.
[97] J. B. Fournier, Europhys. Lett., 43 (1998), 725.
[98] J. B. Fournier, Eur. Phys. J.E, 11 (1999), 261.
[99] M. Hamm and M. M. Kozlov, Eur. Phys. J. B, 6 (1998), 519.
[100] M. Hamm and M. M. Kozlov, Eur. Phys. J. E, 3 (2000), 323.
[101] S. May and A. Ben-Shaul, Biophys. J., 76 (1999), 751.
[102] S. May, Eur. Biophys. J., 29 (2000), 17.
[103] Y. Kozlovsky and M. M. Kozlov, Biophys. J., 82 (2002), 882.
[104] J. A. Killian, I. Salemink, M. R. R. de Planque, G. Lindblom, R. E. Koeppe and D. V. Greathouse, Biochemistry, 35 (1996), 1037.
[105] S. Morein, E. Strandberg, J. A. Killian, S. Persson, G. Arvidson, R. E. Koeppe and G. Lindblom, Biophys. J., 73 (1997), 3078.
[106] P. C. A. van der Wel, T. Pott, S. Morein, D. V. Greathouse, R. E. Koeppe and J. A. Killian, Biochemistry, 39 (2000), 3124.
[107] R. M. Epand, Y. Shai, J. P. Segrest and G. M. Anantharamaiah, Biopolymers (Peptide Science), 37 (1995), 319.
[108] B. Bechinger, Phys. Chem. Chem. Phys., 2 (2000), 4569.
[109] M. Dathe and T. Wieprecht, Biophys. Biochim. Acta., 1462 (1998), 71.
[110] H. W. Huang, J. Phys. II France, 5 (1995), 1427.
[111] M. J. Zuckermann and T. Heimburg, Biophys. J., 81 (2001), 2458.